

The aerodynamic characteristics of twin column, high rise bridge towers

Francesco Ricciardelli[†] and Barry J. Vickery[‡]

*The Boundary Layer Wind Tunnel Laboratory, Faculty of Engineering Science,
The University of Western Ontario, London, Ontario, N6A 5B9, Canada*

Abstract. The high-rise supporting towers of long-span suspension and cable-stayed bridges commonly comprise a pair of slender prisms of roughly square cross-section with a centre-to-centre spacing of from perhaps 2 to 6 widths and connected by one or more cross-ties. The tower columns may have a constant spacing as common for suspension bridges or the spacing may reduce towards the top of the tower. The present paper is concerned with the aerodynamics of such towers and describes an experimental investigation of the overall aerodynamic forces acting on a pair of square cylinders in two-dimensional flow. Wind tunnel pressure measurements were carried out in smooth flow and with a longitudinal intensity of turbulence of 0.10. Different angles of attack were considered between 0° and 90°, and separations between the two columns from twice to 13 times the side width of the column. The mean values of the overall forces proved to be related to the bias introduced in the flow by the interaction between the two cylinders; the overall rms forces are related to the level of coherence between the shedding-induced forces on the two cylinders and to their phase. Plots showing the variation of the force coefficients and Strouhal number as a function of the separation, together with the force coefficients spectra and lift cross-correlation functions are presented in the paper.

Key words: bluff body aerodynamics; aerodynamic interference; wind tunnel testing; aerodynamic forces; bridge towers.

1. Introduction

Wind loads play an important role in the design of towers of cable-stayed and suspension bridges. In particular between the completion of the tower and that of the deck, the pylon is subject to the full wind load but receives very little support from the cables (Scruton and Walshe 1963). This stage, even if it lasts for a short time, can be critical for the pylon.

The assessment of the wind loads on high rise-bridge towers often requires wind tunnel tests. The tests are usually carried out on an aeroelastic model of the tower, and thus have to be considered more as a check since they should be conducted at the end of the design phase.

However, in all the cases where the tower is made of two vertical or nearly vertical columns, connected at different heights through horizontal beams, a first estimate of the wind loads can be obtained through wind tunnel measurements on a sectional pressure model. Moreover, if the contribution of the horizontal elements is neglected, and the tip effect

[†] Research Associate, At present with: Dipartimento di Analisi e Progettazione Strutturale, Univesità di Napoli Federico II, via Claudio, 21-80125 Napoli, Italy

[‡] Professor and Research Director

neglected or taken into account through a correction factor, an estimate of the structural response can be obtained following the method presented in Ricciardelli (1996) and Ricciardelli (1997). The tests are in this case cheaper than in the case in which an aeroelastic model is used, and allow the assessment of the loads without knowledge of the mechanical properties of the structure. This allows to improve the aerodynamics of the structure in the design stage.

The analysis of the wind effects on bridge pylons has been dealt with in a number of papers, many of them presenting case studies. In Shiraishi *et al.* (1986) and in Sakamoto and Haniu (1988) the results of wind tunnel tests aimed at investigating the forces acting on a pair of prisms in tandem or side by side are presented. In Shiraishi *et al.* (1988) and Takeuchi (1990) the effect of corner cuts on rectangular columns in a tandem arrangement is considered, and their effectiveness in reducing the structural response is shown. More recently (Larose *et al.* 1997) the results of full scale measurements on the 254 m high free-standing pylon of the Storebaelt East Bridge were published, pointing out the effects of the aerodynamic interference between the two legs on the structural response.

In a previous paper (Ricciardelli and Vickery 1994) the authors presented the results of a set of wind tunnel tests aimed at investigating the aerodynamic interference between two long cylinders of square cross-section in smooth and turbulent uniform flow and the forces acting on each of the two cylinders. Drag and lift coefficients were presented (mean and rms values), together with their spectra, for different angles of attack and for centre-to-centre distances of 2 to 13 times the side width of the square.

Different behaviours were found, depending on the angle of attack. In particular, for the tandem arrangement, i.e., when the two cylinders are aligned with the flow, and for small values of the angle of attack α (Fig. 1) it was found that the interference between the cylinders, except for very small separations, has a convective nature. The shedding frequency is the same for the two cylinders, and the time lag varies linearly with the separation. Moreover the highest value of the lift cross-correlation function is negative, showing that a vortex sheds from one side of the downstream cylinder when the cylinder is hit on the other side by a vortex coming from the upstream cylinder. For the large angles of attack and for the side by side arrangement the forces acting on the two cylinders appear as the result of the biased flow due to the interference between the cylinders. The lift spectra of the downstream cylinder show two peaks; one is at the same frequency of the peak of the upstream cylinder, while the second is at a lower frequency. The results proved to be in agreement with those

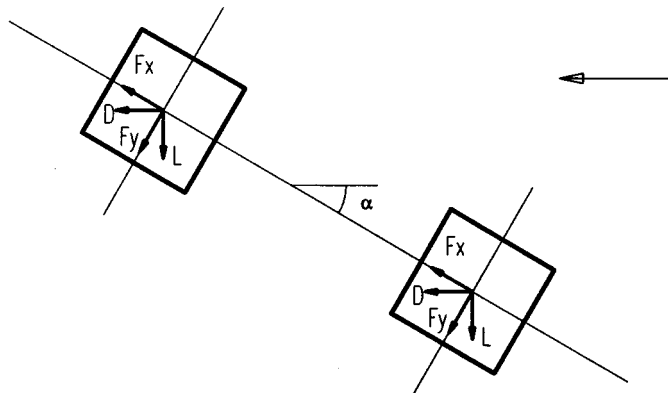


Fig. 1 Force signs

presented in the above referenced papers and in Reinhold *et al.* (1977) and Blessman and Riera (1979).

In the present paper the overall forces acting on a pair of cylinders are investigated. The results presented here constitute an example of the use of pressure measurements to assess the wind loads on bridge pylons, and can be directly used for pylons having columns with a square or nearly square cross-section.

More than in the drag and lift directions, it is useful to have knowledge of the forces acting in the x and y directions (Fig. 1), i.e., the forces in the plane of the tower and in the direction of the bridge axis. Furthermore, although the torque acting on the single cylinder is negligible, the overall torque is relevant, mainly due to the eccentricity of the y forces acting in opposite direction on the two cylinders.

2. Experimental setup

The tests were carried out in Wind Tunnel I at the *Boundary Layer Wind Tunnel Laboratory* of the *University of Western Ontario*. Wind Tunnel I is an open circuit boundary layer wind tunnel with a length of 33 m and a cross-section of 2.44 m of width. The adjustable roof was set at an average height of 1.72 m and was shaped so to obtain a uniform pressure distribution in the tunnel. In order to test in uniform flow, the upstream testing section of the tunnel was used for the tests. The models were placed 7.40 m downstream of the honeycomb grid located at the inlet. The reference Pitot tube was placed at 0.52 m from the roof, and 0.15 m from the centre of the tunnel.

The models consisted of a pair of aluminium cylinders 1.20 m long, with a hollow cross section of 3 cm by 3 cm. The midspan Plexiglas section was fitted on each side with 8 pressure taps of a diameter of 0.89 mm. The two cylinders were horizontally mounted on two circular endplates, that allowed rotation and change of angle of attack, while a slot allowed the displacement of the downstream cylinder to vary the separation (Fig. 2). No evidence of the mounting vibration was noticed on the measured pressure spectra.

The tubing between the pressure taps and the transducers was fitted with restrictors to introduce damping in the dynamic system. The tubing transfer function proved to be almost flat up to frequencies of about 105 Hz. The electrical analogue signal produced by the transducers was analysed through a high speed pressure scanner, and stored as voltage time series.

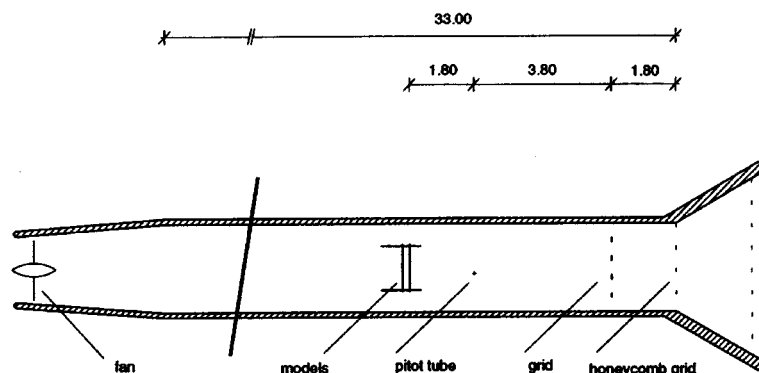


Fig. 2 Sketch of the experimental setup

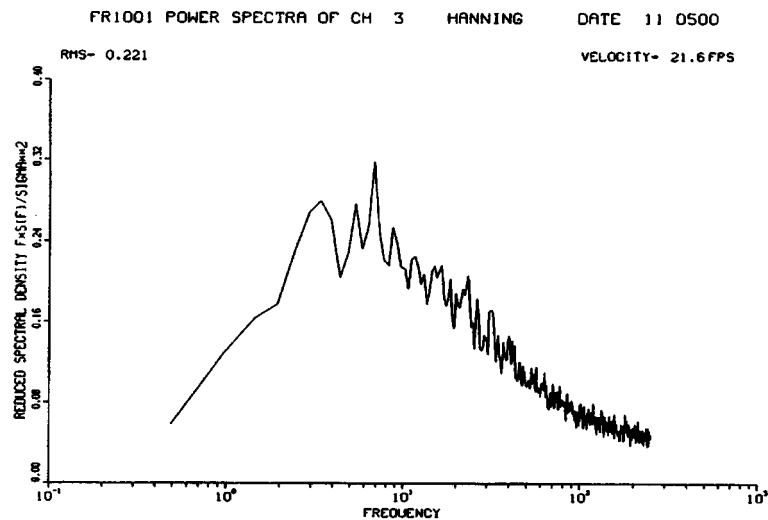


Fig. 3 Reduced spectral density of the longitudinal turbulence, coarse grid exposure

In smooth flow the wind speed was set to 10.7 m/s, that gives a Reynolds number of 22000 if the side of the square section is used as characteristic length. The region where the models were placed was found to be out of the thin boundary layer detected. Longitudinal and lateral intensities of turbulence of 0.004 and 0.003 were measured respectively. The turbulent flow was obtained through the use of a coarse grid made of 14 cm wide bars 55 cm apart, giving a longitudinal intensity of turbulence of 0.10 and an integral scale of the longitudinal turbulence of 0.24 m¹, that is 8 times the side of the square section. In Fig. 3 the spectrum of the longitudinal turbulence is plotted.

Angles of attack of 0°, 7.5°, 15°, 30°, 45°, 60°, 75° and 90° were considered, and separations varying between 2 and 13². The time series were recorded for 256 sec at a sampling frequency of 200 Hz, and the aerodynamic forces were calculated by integration of the pressures.

More details on the experimental setup are given in Ricciardelli (1994).

3. The tandem arrangement

3.1. Smooth flow

For cylinders in tandem arrangement three different behaviours of the flow were observed (Ricciardelli 1994 and Ricciardelli and Vickery 1994), depending on the separation :

- For $s/b < 3$ the two cylinders act as a single body; the separated flow from the upstream cylinder reattaches on the downstream cylinder, the gap flow is almost absent and the wake of the downstream cylinder is narrow. The forces acting on the two cylinders are low (the drag on the downstream cylinder being negative).

¹ The turbulence wave length was calculated, assuming a convective behaviour, as $U \cdot S(0) / 4 \bar{u}^2$, where $S(0)$ is turbulence spectral value at zero, and \bar{u} the rms wind speed.

² By separation it is meant the ratio of the centre-to-centre distance between the two cylinders s to the side b of the square cross-section.

- For $s/b > 3$ the two cylinders interfere with each other; the gap flow is fully developed and the fluctuating drag on the upstream face of the downstream cylinder is partly due to low frequency turbulence of the gap flow and partly to the oncoming vortices. Oncoming vortices from the upstream cylinder trigger vortex shedding from the downstream cylinder, but the changes that the downstream cylinder causes to the wake of the upstream cylinder make the forces acting on the upstream cylinder be slightly different in magnitude from those found for a single cylinder.
- For $s/b \gg 3$ the upstream cylinder is not influenced by the downstream cylinder; the downstream cylinder is in a wake flow and therefore the forces acting on it are affected by the reduced wind speed and increased level of turbulence.

For all separations considered the lift spectra are narrowband, and the cross-correlation between the lift forces on each cylinder is high (Fig. 4). In all cases vortex shedding occurs at the same rate for the two cylinders (Fig. 5), although the shedding frequency varies with the separation.

The maximum values of the cross-correlation functions are always negative, and the time lag between the vortex shedding from the two cylinders varies linearly with the separation. This suggests that the interaction between the two cylinders has a convective nature, and that vortices are shed from the downstream cylinder when hit on the opposite side by a vortex coming from the upstream cylinder.

In Fig. 6 the shedding lag³ is plotted as a function of the separation; the points can be very

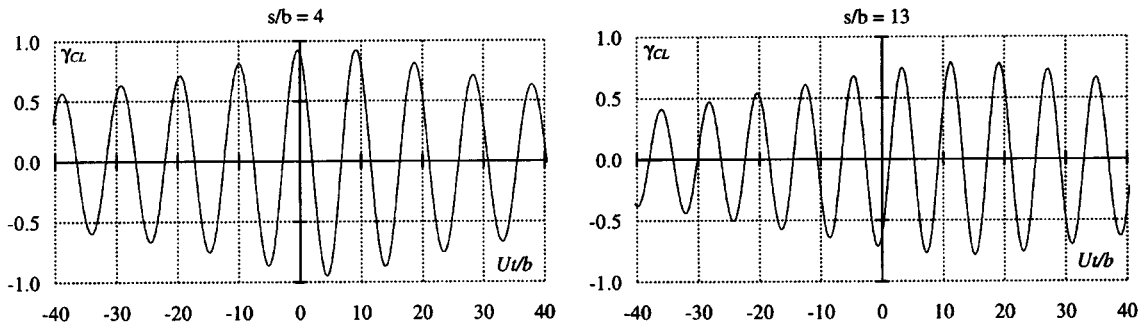


Fig. 4 Lift cross-correlation for the tandem arrangement in smooth flow

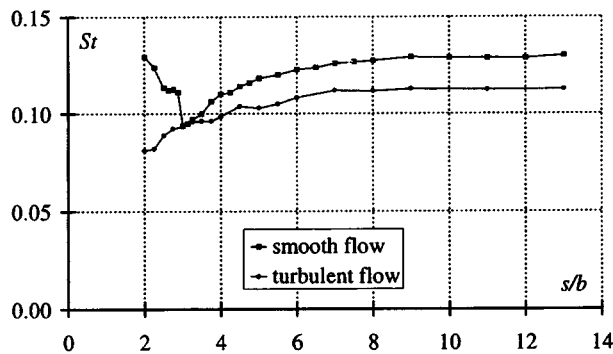


Fig. 5 Strouhal number for the tandem arrangement

³ The shedding time lag is defined as the average time difference between lift peaks on the upstream and downstream cylinder.

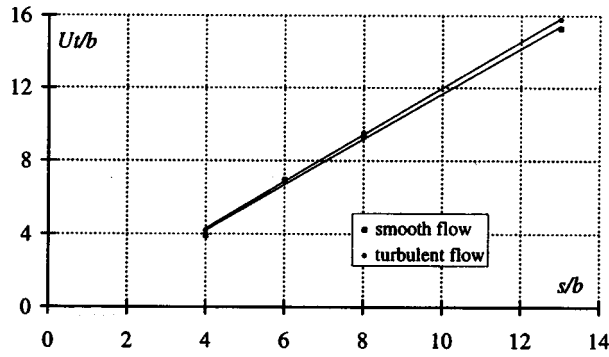


Fig. 6 Shedding lag for the tandem arrangement

well fitted by a straight line, showing a convective velocity of vortices equal to the 80% of the reference wind velocity.

This behaviour suggests that when the separation is :

$$\frac{s}{b} = \frac{n}{St} \cdot \frac{U_v}{U} \quad (1)$$

U and U_v respectively being the mean reference wind velocity and the convective velocity of vortices, $St = f_s b / U$ the Strouhal number and n an integer number, vortices shed in opposite phase from the two cylinders.

Moreover, when:

$$\frac{s}{b} = \frac{n + 0.5}{St} \cdot \frac{U_v}{U} \quad (2)$$

vortices shed in phase from the two cylinders.

The mean overall torque and y -direction force are zero because of the symmetry of the flow, and Eqs. (1) and (2) give the separations at which the maximum rms values of the torque and of the y -direction force occur.

The forces and the torque acting on the pair of cylinders can be expressed in terms of the non-dimensional coefficients :

$$C_{F_x} = \frac{F_{x1} + F_{x2}}{\frac{1}{2} \rho U^2 b} \quad (3)$$

$$C_{F_y} = \frac{F_{y1} + F_{y2}}{\frac{1}{2} \rho U^2 b} \quad (4)$$

$$C_w = \frac{W}{\frac{1}{2} \rho U^2 b s} \quad (5)$$

F_{x1} , F_{x2} , F_{y1} , F_{y2} and W respectively being the x -direction and the y -direction forces acting on the two cylinders and the overall torque. The torque is calculated with respect to the centre of the overall cross-section, giving :

$$W = W_1 + W_2 + (F_{y1} - F_{y2}) \frac{s}{2} \tag{6}$$

where W_1 and W_2 are the torques acting on each cylinder. Mean and rms force coefficients will be considered in the paper, calculated, through Eqs. (3), (4) and (5), from the mean and rms values of the aerodynamic forces.

Figs. 7 and 8 show the variation of the rms torque and y -direction force coefficients with the separation. For very small separations ($s/b < 3$) both the coefficients have very low values, mainly due to the low value of the fluctuating lift on the two cylinders. For larger separations the lift force is relevant and so is the torque and the overall y -direction force. The variation of the y -direction force and torque coefficients is related to the changes occurring in the phase between the vortex shedding from the two cylinders with changing separation. The two diagrams show an undulating behaviour, with maximum values of the one corresponding to minimum values of the other. Maximum values of the overall y -direction force occur for separations at which vortices shed in phase from the two cylinders. Maximum values of the torque occur for separations at which vortices shed in opposite phase from the two cylinders.

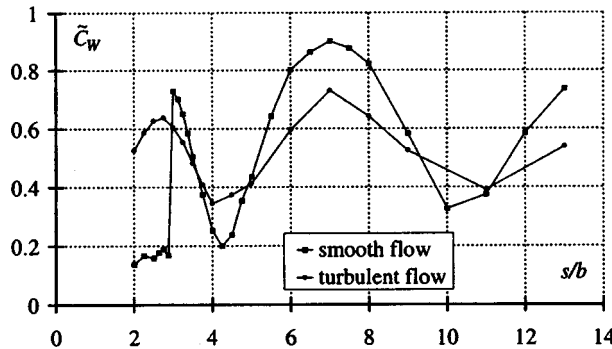


Fig. 7 Rms torque coefficients for the tandem arrangement

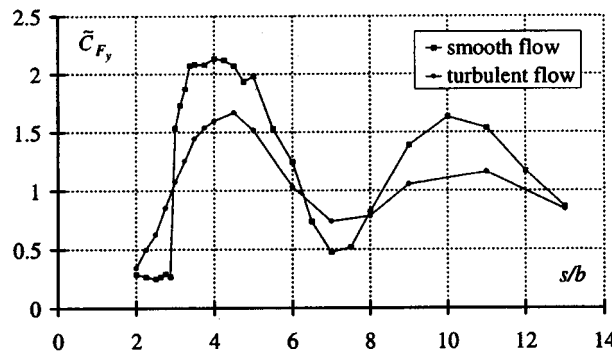


Fig. 8 Rms F_y coefficients for the tandem arrangement

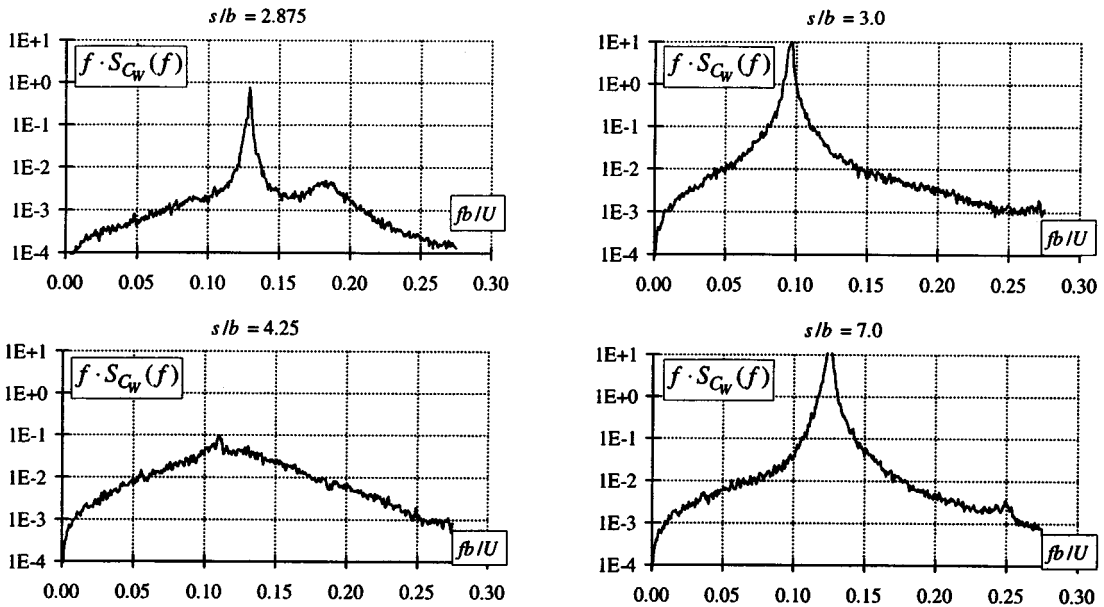


Fig. 9 Torque coefficient spectra for the tandem arrangement in smooth flow

As the separation increases, the reduction in coherence brings a reduction in the amplitude of fluctuation of the two coefficients.⁴

The same conclusions can be drawn from the spectra of the torque and of the *y*-direction force. In Fig. 9 the spectra of the torque coefficient are plotted, for separations of $s/b = 2.875$, $s/b = 3.0$, $s/b = 4.25$ and $s/b = 7.0$. For a separation of $s/b = 2.875$ the spectral values are generally low, with a narrowband peak at the shedding frequency. For larger separations the spectra show the same background component, although a high peak exists at the shedding frequency for separations $s/b = 3.0$ and $s/b = 7.0$, that does not appear for a separation $s/b = 4.25$, in agreement with the predicted behaviour.

The mean force in the *x* direction has low values for separations $s/b < 3$, due to the

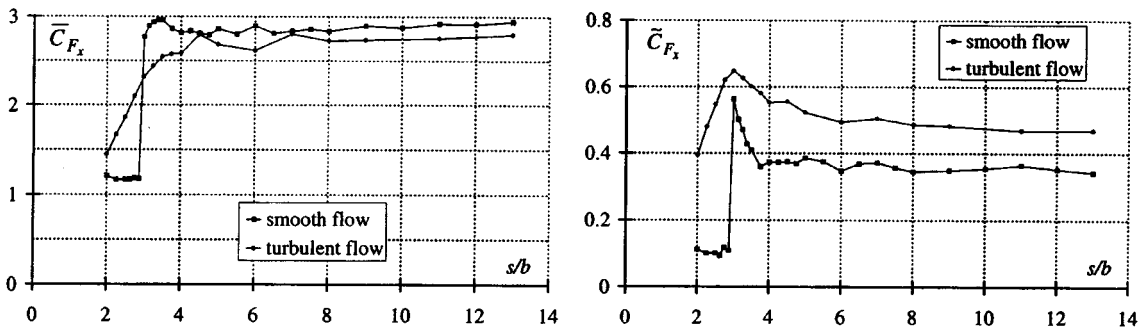


Fig. 10 F_x coefficients for the tandem arrangement

⁴ All the forces were measured on stationary cylinders and thus do not include motion induced forces. A dependency of the cross-correlation of the shedding induced forces on the amplitude of vibration and phase shift is expected in the case of vibrating cylinders.

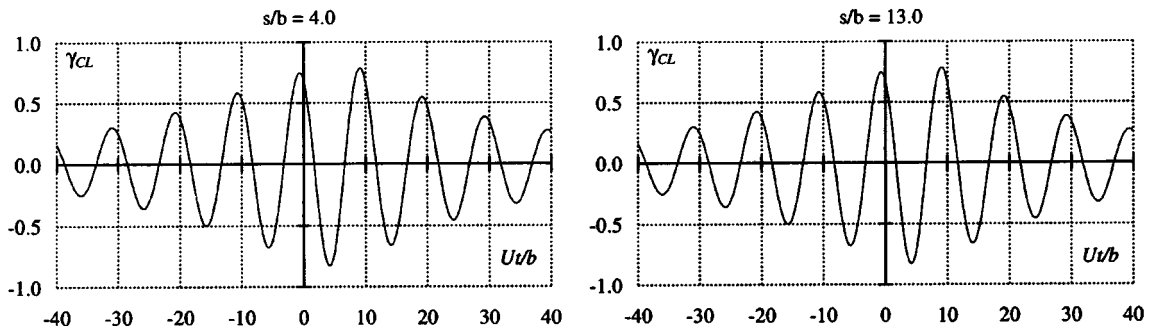


Fig. 11 Lift cross-correlation for the tandem arrangement in turbulent flow

negative drag on the downstream cylinder (Fig. 10). At $s/b = 3$ a sudden increase occurs, due to the change in the flow pattern; the mean F_x coefficient rises to a much higher value, that stays near that value for all spacings considered. The rms F_x coefficient too (Fig. 10) has low values for $s/b < 3$, however after the discontinuity it has a maximum value, due to the high level of turbulence of the gap flow; the coefficient then decreases in the range $3 < s/b < 4$, and is constant for separations greater than 4.

3.2. Turbulent flow

Almost all the features found in smooth flow were found in turbulent flow, however, instead of a sudden discontinuity, a gradual transition takes place between the two different behaviours pointed out for the smooth flow as $s/b < 3$ and $s/b > 3$. For very small separations the mean drag coefficient has small values. The Strouhal number (Fig. 5) is again the same for the two cylinders and monotonically increases with the separation. The cross-correlation (Fig. 11) between lift forces on the two cylinders is lower than in smooth flow, and more rapidly decaying with both time and spacing; however the interaction has still a convective nature and the time lag between the shedding of vortices from the two cylinders is again linear with the separation (Fig. 6). A convective velocity of vortices of 78% that of the mean flow was found in this case.

The plots showing the variation of the rms torque and y -direction force coefficients (Figs. 7 and 8) with the separation are similar to those presented for a smooth flow. The two diagrams again alternate maximum and minimum values as the separation increases, although the amplitude of fluctuation is smaller and the scatter higher than in smooth flow, due to the lower coherence between the shedding of vortices from the two cylinders.

The mean x -direction force (Fig. 10) gradually increases in the range $2 < s/b < 5$, and remains constant after that. The fluctuating part of the x -direction force increases to a maximum value for $s/b = 3$, and decreases after that.

4. Arrangements with small angles of attack

For angles of attack smaller than 30° features similar to those found for the tandem arrangement were observed. The downstream cylinder is again in the wake of upstream cylinder, however the fact that it is not in the centre of the wake and that, as the separation increases, the distance from the centre of the wake increases, makes the forces variation with

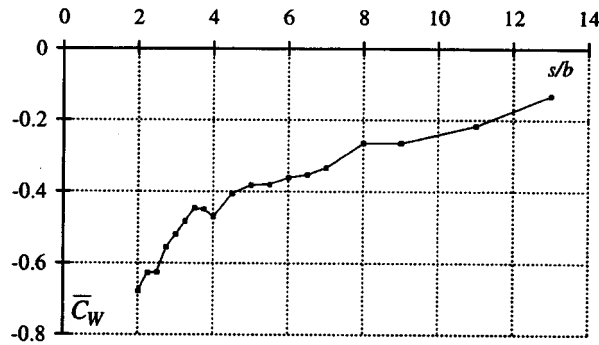


Fig. 12 Mean torque coefficients at 15° in smooth flow

separation less regular than in the tandem arrangement.

For very small separations the two cylinders can still act like a single body, although this feature becomes less evident as the angle of attack increases, and vortices shed from the two cylinders at the same rate.

Due to the convective nature of the interaction between the two cylinders, the variation of the rms torque and y-direction force with the separation features the same alternation between maximum and minimum values, found for the tandem arrangement. However the amplitude of fluctuation decreases as the angle of attack increases.

On the other hand the mean values of the torque and y-direction force start to be significant. The highest values of the mean torque are found for small separations and for angles of attack of 7.5° and 15°, both in smooth and turbulent flow (Fig. 12). In these cases the bias introduced in the flow around the downstream cylinder by the upstream cylinder causes mean lift forces of opposite sign on the two cylinders; the result of which is a mean twisting action on the pair of cylinders.

The mean value of the y-direction force increases as the angle of attack increases, as the component of the drag in the y direction increases. However for an angle of attack of 7.5°, and for small separations, high values were found (Fig. 13); this can be explained by the reattachment of the separated flow from the upstream cylinder on the downstream cylinder. This causes strong lift forces on the downstream cylinder, and thus an high y-direction force on the pair of cylinders.

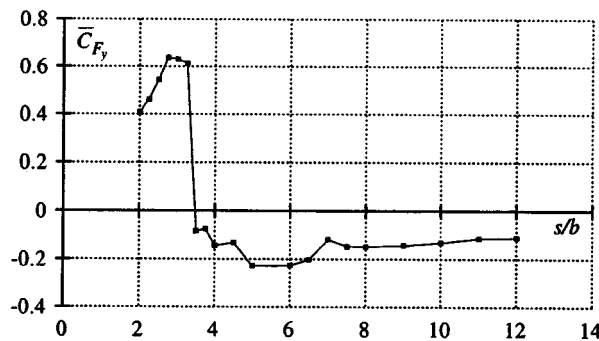


Fig. 13 Mean F_y coefficients at 7.5° in smooth flow

5. The side by side arrangement

5.1. Smooth flow

When the cylinders are in the side by side arrangement ($\alpha = 90^\circ$), the symmetry of the geometric arrangement suggests that the flow and the aerodynamic forces be symmetric too. However, for small separations ($s/b < 2.5$) the symmetric flow pattern proves to be unstable, and a non-symmetric flow occurs. Two non-symmetric flow patterns are possible, each being symmetric with respect to the other, and an alternation between them takes place. However small imperfections in the geometric setup caused one of the two flow patterns to be more likely to occur than the other, which brought two different values of the time averaged mean and rms forces acting on the two cylinders.

For larger spacings, the flow, and thus the forces, are globally symmetric. However the flow is still biased for each of the two cylinders. There results a mean attractive lift and a strong component of the shedding-induced forces in the drag direction.

Vortices are shed at the same frequency from the two cylinders for all separations (Fig. 14). However for small separations the two cylinders act as a single body, with vortices shedding only from the outer sides. The lift cross-correlation functions (Fig. 15) show, when the separation is small ($s/b < 2.5$), a lower and more rapidly decaying coherence in the vortex shedding than for larger separations ($s/b > 2.5$). As the separation increases the coherence between lift forces reduces, although the correlated part of these forces is still in phase. The maximum value of the correlation is negative and corresponds to a zero time lag, suggesting that vortices shed symmetrically from the external and then internal faces of the cylinders.

For the side by side arrangement the y -direction forces are drag forces. The mean value of the y -direction force is almost constant with the separation (Fig. 16) and equal to the sum of the drag forces acting on the two cylinders; for separations $s/b < 2.5$ its value is lower due to the reduction in drag resulting from the biased flow. For the same reason the mean torque (Fig. 17) has large values when the separation is small and tends to zero as the separation increases.

Both the rms torque and y -direction force (Figs. 16 and 17) have a maximum value for $s/b = 2.5$, corresponding to the maximum value in the fluctuating drag.

On the torque spectra (Fig. 18) a clear peak can be seen only for very small separations, i.e., when the rms torque is due to a difference in magnitude between the well correlated rms drag

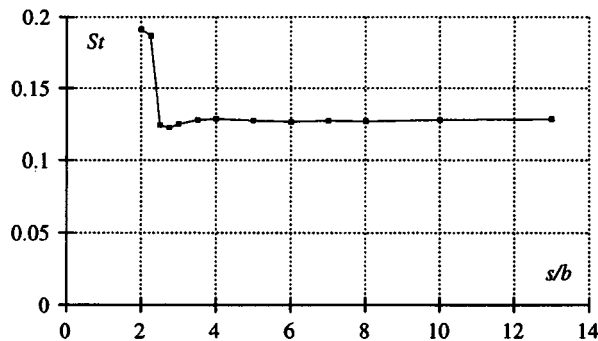


Fig. 14 Strouhal number at 90° in smooth flow

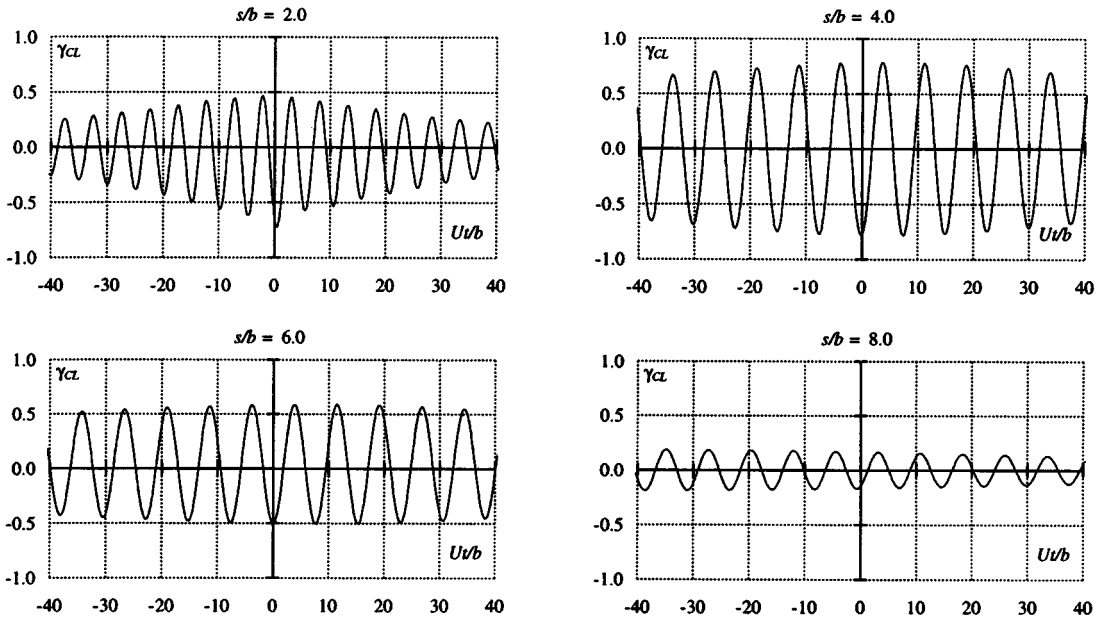


Fig. 15 Lift cross-correlation at 90° in smooth flow

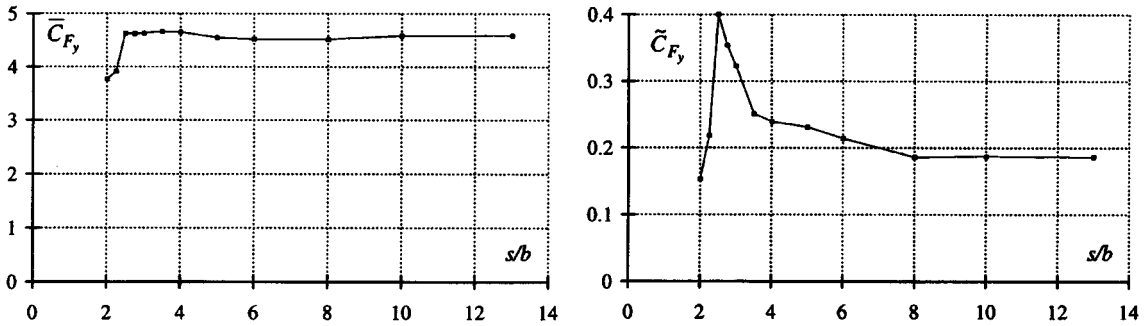


Fig. 16 F_y coefficients at 90° in smooth flow

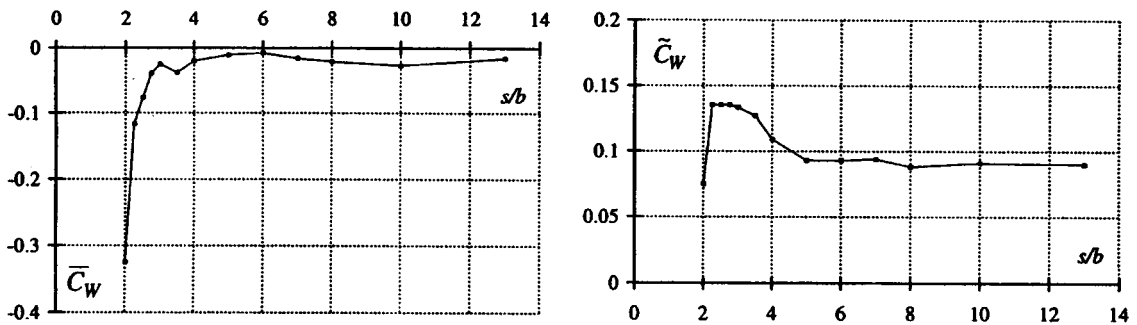


Fig. 17 Torque coefficients at 90° in smooth flow

forces. For larger separations, i.e., when the rms torque is due to the lack of coherence between forces of the same magnitude, the peak is much smaller if not non-existent.

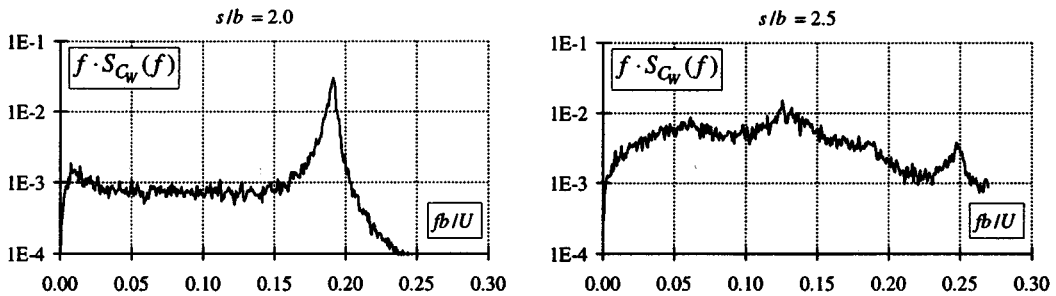


Fig. 18 Torque spectra at 90° in smooth flow

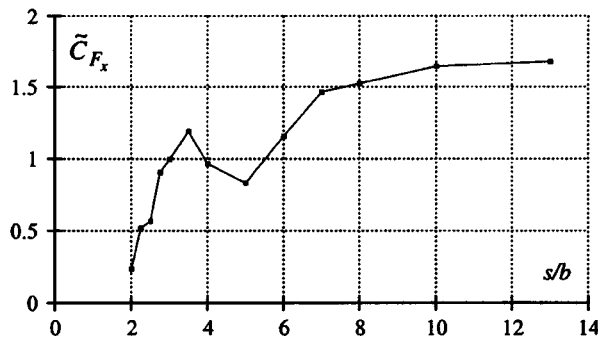
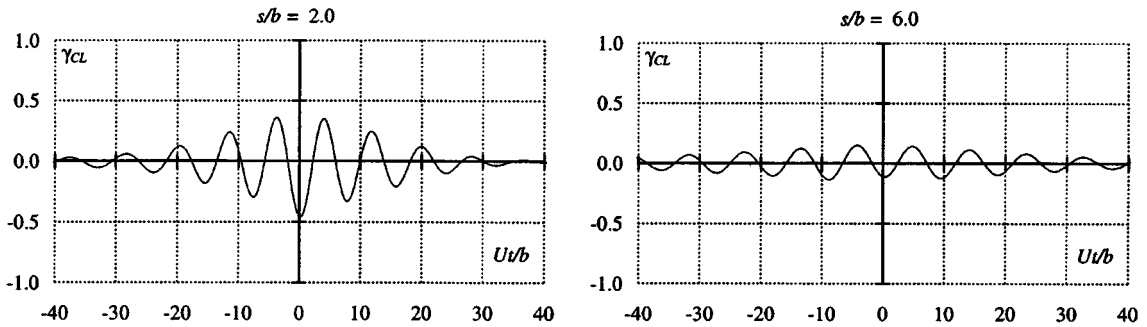
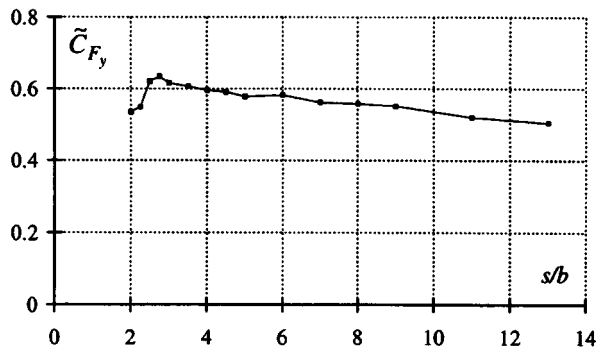


Fig. 19 Rms F_x coefficients at 90° in smooth flow

The mean force in the x direction (lift) is almost nil when the flow is symmetric ($s/b > 2.5$), while it has non-zero values for very small separations. The fluctuating part of the x -direction force (Fig. 19) increases when the separation is in the range $2 < s/b < 3.5$ due to an increase in the magnitude of the shedding-induced forces; a reduction takes place in the range $3.5 < s/b < 5$, due to the increase in coherence between the vortex shedding from the two cylinders (vortices shed at the same time from opposite sides of the cylinders, result in a low global force); the reduction in coherence between the lift forces on the two cylinders causes, for separations $s/b > 5$ a further increase in the overall rms lift.

5.2. Turbulent flow

In turbulent flow features similar to those found in smooth flow for $s/b > 2.5$ were found, although the presence of a biased flow at small separations was not detected. The coherence of lift forces is much lower, and its decay with time and separation is faster (Fig. 20); however the correlated part is still in opposite phase, as it is in smooth flow. The mean y -direction force is the sum of the drag forces acting on the two cylinders, while the torque is almost zero for all spacings. The rms y -direction force (Fig. 21) slightly decreases with the separation with values globally higher than in smooth flow; the rms torque also has higher values than in smooth flow, and slightly increases with separation. The absence of a well pronounced peak on the spectra shows how the fluctuating part of the torque is due to the lack of coherence in the turbulence more than to different vortex-induced forces. Like in smooth flow the mean x -direction force is almost zero; its rms value increases with separation, due to the reduction in the coherence between vortex shedding from the two cylinders.

Fig. 20 Lift cross-correlation at 90° in turbulent flowFig. 21 Rms F_y coefficients at 90° in turbulent flow

6. Arrangements with large angles of attack

When the transversal distance between the two cylinders is close to or greater than the longitudinal distance, the characteristics of the forces acting on the downstream cylinder are no longer related to the wake flow, but more to a biased flow due to the presence of the upstream cylinder. The most evident result of that is the existence, for the downstream cylinder and for small and medium separations, of two peaks on the lift spectra and, for high separations, of one peak at a frequency different from that of the upstream cylinder. In Fig. 22 the variation of the Strouhal number with the separation is shown, for an angle of attack of 45° ; two curves are shown, one corresponding to the peak in the lift spectrum of the upstream cylinder, the second to the secondary peak on the lift spectrum of the downstream cylinder.

A convective interference between the two cylinders can still be seen from the lift cross-correlation functions (Fig. 23), although the coherence between the forces is much lower than in the previous cases, and strongly decaying with time.

Both in smooth and in turbulent flow the mean torque has a maximum value for small separations (Fig. 24), i.e., when the biased flow causes mean y -direction forces on the two cylinders of different magnitude. As the separation increases the bias reduces and the torque goes to zero. On the other hand the rms torque increases as the separation increases, due to a reduction in coherence between the shedding-induced forces on the two cylinders.

The y -direction forces are almost drag forces, and therefore the mean value is, except for very small separations, constant with separation but increases with the angle of attack.

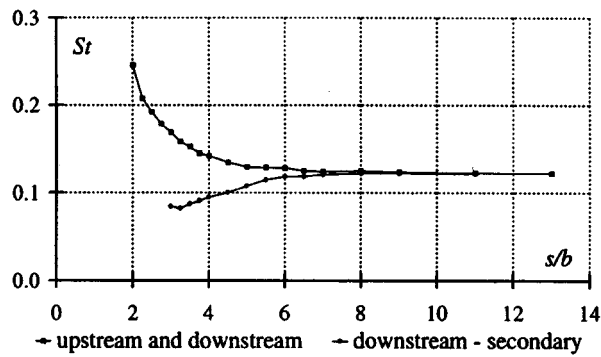


Fig. 22 Strouhal number at 45° in smooth flow

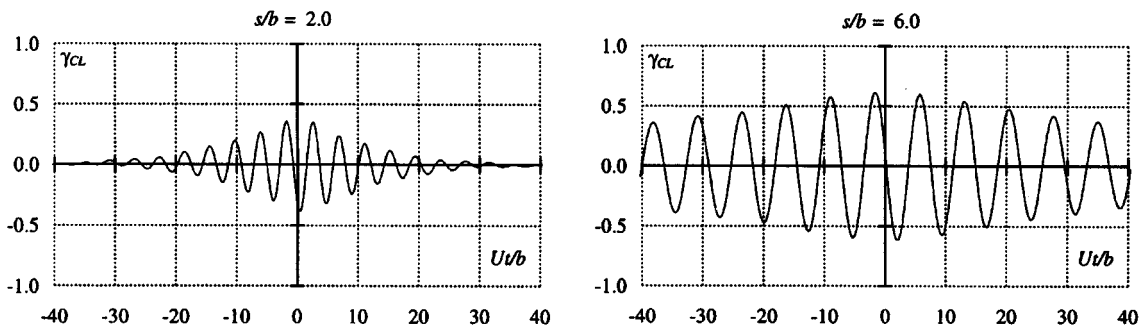


Fig. 23 Lift cross-correlation at 45° in smooth flow

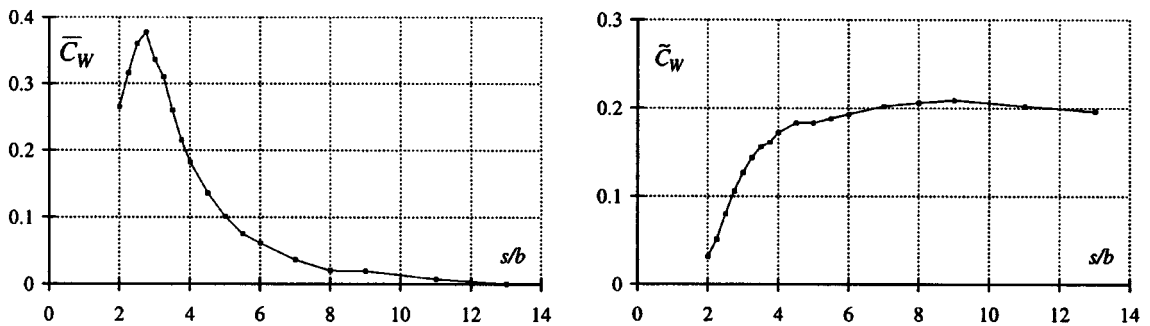


Fig. 24 Torque coefficients at 60° in smooth flow

The mean and rms x -direction forces generally increase with the separation.

7. Conclusions

Although a broad range of separations was considered in the tests, in most of the cases, for a bridge tower, the separation ratio is in the range $4 < s/b < 5$.

The mean y -direction forces are strongly affected by the angle of attack, i.e., by the angle between the y direction and the drag direction. As the angle of attack increases the angle between the y direction and the drag direction reduces and the mean force increases.

The mean torque is due to the biased flow, and has its highest values, both in smooth and

turbulent flow, for an angle of attack of 15° .

The magnitude of the fluctuating part of the aerodynamic forces is mainly related to the level of coherence and to the synchronisation between the shedding-induced forces. For the tandem arrangement and for small angles of attack, the coherence is high and the shedding from the downstream cylinder is triggered by the oncoming vortices. In these cases the highest values of the force coefficients are given for separations such that vortices shed in phase (maximum y force) or in opposite phase (maximum torque). The highest coherence in vortex shedding is for a 0° angle of attack; in this case, for separations in the technical range, the rms y -direction force has a maximum value, while the rms torque has lower values.

For large angles of attack, the highest values of the rms force coefficients occur for large separations, due to the lower level of coherence of the shedding-induced forces.

References

- Blessmann J., Riera J.D. (1979), "Interaction effects in neighbouring tall buildings", *Proc. 5th Int. Conf. Wind Engng.*, Fort Collins, Colorado, 381-395.
- Larose G., Zasso A., Melelli S. and Casanova D. (1997), "Field measurements of the wind-induced response of a 254 m high free-standing bridge pylon", *2nd EACWE*, Genova, Italy, 1553-1560.
- Reinhold T.A., Tieleman H.W., Maher F. (1977), "Interaction of square prisms in two flow fields", *J. Ind. Aero.*, **2**(3), 223-241.
- Ricciardelli F. (1994), "Aerodynamics of a pair of square cylinders", M.E.Sc. Thesis, Faculty of Engineering Science, The University of Western Ontario, London, Ontario, September.
- Ricciardelli F., Vickery B.J. (1994), "Wind loads on a pair of long prisms of square cross-section", *IN-VENTO-94, Proc. 3rd Nat. Italian Conf. Wind Engng.*, Roma, October, 101-120.
- Ricciardelli F. (1996), "Wind induced vibrations of high-rise bridge towers", *Eurodyn '96, Proc. 3rd European Conf. on Struct. Dynamics*, Firenze, Italy, June, 325-332.
- Ricciardelli F. (1997), "Prediction of the response of suspension and cable-stayed bridge towers to wind loading", *J. Wind Engng. Ind. Aero.* **64**, 145-159.
- Sakamoto H., Haniu H. (1988), "Aerodynamic forces acting on two square prisms placed vertically in a turbulent boundary layer", *J. Wind Engng. Ind. Aero.*, **31**, 41-66.
- Scruton C., Walshe D.E. (1963), "An investigation of the aerodynamic stability of the towers proposed for the River Severn Suspension Bridge," *NPL Aero Report 1052*.
- Shiraishi N., Matsumoto M., Shirato H., Ishizaki H. (1988), "On aerodynamic stability effects for bluff rectangular cylinders by their corner-cut", *J. Wind Engng. Ind. Aero.*, **28**, 371-380.
- Shiraishi N., Matsumoto M., Shirato H. (1986), "On aerodynamic instabilities of tandem structures", *J. Wind Eng. Ind. Aero.*, **23**, 437-447.
- Takeuchi T. (1990), "Effects of geometrical shape on vortex-induced oscillations of bridge tower", *J. Wind Eng. Ind. Aero.*, **33**, 359-368.

Notations

b	= Characteristic dimension of the cross-section (side width of the square)
C_w	= Torque coefficient
C_{F_x}	= Force coefficient in the x direction
C_{F_y}	= Force coefficient in the y direction
D	= Drag force (per unit length)
F_x	= Force in the x direction (per unit length)
F_y	= Force in the y direction (per unit length)
L	= Lift force (per unit length)
s	= Centre-to-centre distance between the cylinders

$S_{c_w}(f)$	= Spectrum of the torque coefficient
St	= Strouhal number ($=fb/U$)
t	= Time
U	= Reference mean velocity
U_v	= Convective velocity of vortices
W	= Torque (per unit length)
α	= Angle of attack
$\gamma_{c_L}(t)$	= Lift coherence function ($=R_{L_1L_2}(t)/\tilde{L}_1\tilde{L}_2$)
ρ	= Air density
$-$	= mean value
\sim	= rms value

(Communicated by Giovanni Solari)